Journal of Hazardous Materials 285 (2015) 581–588

Contents lists available at ScienceDirect

Journal of Hazardous Materials

journal homepage: www.elsevier.com/locate/jhazmat

Characterization and selection of biochar for an efficient retention of tricyclazole in a flooded alluvial paddy soil

Manuel García-Jaramillo[a,*], Lucía Cox[a], Heike E. Knicker[a], Juan Cornejo[a], Kurt A. Spokas[b], M.Carmen Hermosín[a]

[a] Instituto de Recursos Naturales y Agrobiología de Sevilla (IRNAS-CSIC), P.O. Box 1052, 41080 Seville, Spain
[b] United States Department of Agriculture–Agricultural Research Service, 1991 Upper Buford Circle, Saint Paul 55108, MN, USA

HIGHLIGHTS

- Biochar CEC was inversely correlated with HTT.
- Enhanced aromaticity was associated to an improved biochar adsorption of tricyclazole.
- The SSA of the biochars was inversely correlated with DOC contents.
- Adsorption of tricyclazole was related to high SSA and low DOC content of biochars.
- The use of AC and biochar in conjunction provides the slow release of tricyclazole.

GRAPHICAL ABSTRACT

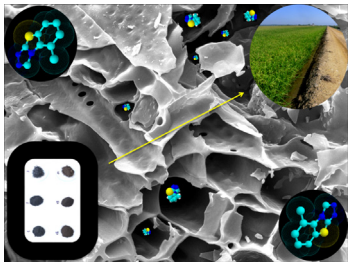

ARTICLE INFO

Article history:
Received 4 August 2014
Received in revised form 23 October 2014
Accepted 29 October 2014
Available online 11 November 2014

Keywords:
Fungicide
Dissolved organic matter;
Specific surface area
^{13}C NMR spectroscopy
Polarity index
Adsorption

ABSTRACT

Biochars, from different organic residues, are increasingly proposed as soil amendments for their agronomic and environmental benefits. A systematic detection method that correlates biochar properties to their abilities to adsorb organic compounds is still lacking. Seven biochars obtained after pyrolysis at different temperatures and from different feedstock (alperujo compost, rice hull, and woody debris), were characterized and tested to reveal potential remedial forms for pesticide capture in flooded soils. Biochar properties were determined by nuclear magnetic resonance (NMR) spectroscopy, Fourier transform infrared spectroscopy, specific surface area (SSA) assessment and scanning electron microscopy. In addition, dissolved organic matter (DOM) from these biochars was extracted and quantified in order to evaluate the effect on pesticide sorption. The biochars from alperujo compost presented very high affinity to the fungicide tricyclazole (55.9, 83.5, and 90.3% for B1, B4, and B5, respectively). This affinity was positively correlated with the pyrolysis temperature, the pH, the increased SSA of the biochars, and the enhanced aromaticity. Sorptive capacities were negatively related to DOM contents. The amendment with a mixture of compost and biochar endows the alluvial soil with high sorptive properties (from $K_{fads(soil)}$ = 9.26 to $K_{fads(mixture)}$ = 17.89) without impeding the slow release of tricyclazole.

1. Introduction

Rice production under conventional flooded conditions has been associated with both environmental and health risks, such as pesticide contamination of soil and water. The use of organic residues

* Corresponding author. Tel.: +34 95 4624711; fax: +34 95 4624002.
E-mail address: mgarcia@irnas.csic.es (M. García-Jaramillo).

http://dx.doi.org/10.1016/j.jhazmat.2014.10.052
0304-3894/

as soil amendments increases the content of soil organic matter (SOM) and thus, improves not only their physical and chemical properties, but also the adsorption of pesticides [1–3]. Due to the need to reduce greenhouse gas emissions and its potential for carbon sequestration [4,5], biochar has been suggested as a soil amendment [6–8]. These residues, generated by pyrolysis, are expected to be biochemically highly recalcitrant but greatly heterogeneous in their chemical composition and physical properties [9,10]. Recently, the characterization of biochars for their use as soil amendment has been an important research focus [11–13]. Biochar has been reported to enhance plant nutrient levels [14,15], to improve soil water retention [16] and to augment microbial activity [17]. Reduced leaching of pesticides by adsorption to biochars has also been reported [18–20]. Surface properties and the physical and chemical structure of biochars are largely controlled by pyrolysis conditions and feedstock, as it has been shown in numerous publications [21,22]. Sorption of organic pesticides to biochar exceeds that to humic acid and SOM [23,24]. Consequently, soil amendment with biochar can have both a positive and a negative effect on pesticide behavior. When sorption is increased, leaching is decreased, minimizing the risk of drainage water contamination [25]. Biochar can significantly contribute to the sorption and sequestration of organic contaminants such as, pesticides in soil due to its special physicochemical properties, as it has been previously described for other fungicides [26].

Tricyclazole is a systemic fungicide, widely used in rice production under paddy field conditions, effective against *Pyricularia oryzae* and other fungus. The recommended dose of application is 0.3 Kg Ha^{-1} and crop cycle. The potential environmental risk of this pesticide is high because of its extended persistence in the soil–water system [27,28]. Its half-life goes from 4 to 17 months in laboratory assays, and approximately 6 months in the field [29]. Also, it does not readily hydrolyze in the environment and it is stable at 51 °C without volatilization. Among the toxic effects of tricyclazole was described its strong interaction with the β-cyclodextrin and human serum albumin [30], reacting by inclusion and forming a new compound. Substance accumulation, in the human body, is likely and may cause some concern following repeated or long-term occupational exposure. Tricyclazole has been included in the US-Maine chemicals of high concern list as carcinogen [WR1].[1] Long term exposure to high dust concentrations may cause changes in lung function, i.e., pneumoconiosis; caused by particles less than 0.5 micron penetrating and remaining in the lung. The sorption capacity of several biochars was studied in order to select the most suitable for the retention of tricyclazole in a water saturated soil. In addition, we tested the possible application of a combined amendment based on a mixture of biochar and alperujo compost, both of them produced from an agro residue of the olive oil industry (alperujo).

2. Materials and methods

2.1. Soil, amendments, and fungicide

The alluvial soil (ALU) used in this work, classified as a Fluvisol [31] (Xerofluvent), was collected in the Guadalquivir river valley from the research station La Hampa (37°17′30″N–06°04′50″W), Coria del Río, Spain. Soil was transported to the laboratory and stored at 4 °C until experiments were carried out. Alperujo, which is the residue of olive oil production, was composted with straw and sheep manure. This alperujo compost (AC) was produced in the research station IFAPA-Centro Venta del Llano, Jaén (Spain) in 2013. Biochars were prepared from different feedstock with a thermal decomposition process at various temperatures under oxygen-limited conditions. To obtain the biochars, the feedstock was placed in ceramic crucibles fitted with a tight-fitting ceramic lid, and then put into an electric furnace (muffler) at the target temperature. The product was ground to a size of less than 0.2 mm. Feedstock and pyrolysis conditions are described in Table 1.

Table 1
Feedstock and processes used to produce the studied biochars.

Feedstock and temperature of production	Abbreviation	Code
Alperujo compost, 400 °C, 2 h	BAC_400	B1
Rice hull (RH), 400 °C, 2 h	BRH_400	B2
Alperujo compost + RH (50:50), 400 °C, 2 h	BAC + BRH_400	B3
Alperujo compost, 550 °C, 2 h	BAC_550	B4
Alperujo compost, 700 °C, 2 h	BAC_700	B5
Hardwood sawdust (HS), 500 °C	BHS	B6
Wood pellet (WP), 700 °C	BWP	B7

Analytical grade tricyclazole (≥97% purity) was supplied by Dr. Ehrenstorfer GmbH (Augsburg, Germany). Its water solubility was 596 mg L^{-1} (20 °C), its GUS (groundwater ubiquity score) leaching potential index was 4.89, and molecular mass 189.24 g mol^{-1} [29]. With this compound we prepared the initial pesticide solutions, which were used as external standards for the pesticide analysis and to carry out all the experimental assays.

2.2. Physical and chemical analysis of soil and amendments

The soil texture, determined by sedimentation using the pipette method [32,33] revealed a relative contribution of sand, silt, and clay of 19.8%, 43.7%, and 36.4%, respectively. The organic matter content was determined according to Walkley and Black [34] and the total nitrogen by the Kjeldahl [35] method. Soil pH and electrical conductivity were measured in a 1:2.5(w/v) soil/deionized water mixture. Physical and chemical properties of the soil, the amended soil are shown in Table 2. The elemental composition (C, H, and N) of the biochars was analyzed by a high-temperature combustion method (Elementar Vario EL, Hanau, Germany). Major cations and CEC were assessed by exchange with 1 M ammonium acetate. Their pH and electrical conductivity were measured in a 1:5(w/v) biochar/deionized water mixture. Dissolved organic carbon (DOC) and dissolved organic nitrogen (DON) from the biochars were obtained by aqueous extraction with calcium chloride (5 mM) and determined with a total organic carbon analyzer (TOC-V_{CPH}, Shimadzu, Kyoto, Japan) connected to a nitrogen unit. All the physical and chemical data obtained from the biochars analysis are presented in Table 3.

2.3. Functional and molecular characterization of biochars

The specific surface area (SSA) of the biochars was determined by nitrogen surface adsorption at 77.35 K in an ASAP 2420 system (Micromeritics). Isotherms were interpreted by the Brunauer–Emmett–Teller (BET) equation [36]. The FT-IR spectra were recorded in the 650–4500 cm^{-1} region using a Jasco FT-IR-6300 spectrometer (Fig. S1, Appendix A). The FT-IR spectral peak

Table 2
Physical and chemical properties of the soil, compost, and amended soil used in the sorption experiments.

Samples	O.M.(%)	N(%)	pH	EC(mS/cm)
Alluvial soil (ALU)	2.38	0.14	8.22	0.16
Alperujo compost (AC)	55.12	1.72	8.91	3.54
ALU + AC (2%)	3.22	0.17	8.23	0.22
ALU + B4 (2%)	2.53	0.15	8.34	0.23
ALU + AC (1%) + B4 (1%)	2.55	0.16	8.27	0.23

[1] [WR1] http://datasheets.scbt.com/sc-237282pdf.

Table 3
Physical and chemical properties of the biochars obtained. Ash content was evaluated at 540 °C. B1(BAC_400); B2 (BRH_400); B3 (BAC + BRH_400); B4 (BAC_550); B5 (BAC_700); B6 (BHS); B7 (BWP).

Code	pH(1:5)	CEC(cmol Kg^{-1})	Ash(mg g^{-1})	N(mg g^{-1})	C(mg g^{-1})	C/N	C/H	S.S.A. (m^2 g^{-1})	DOC (mg L^{-1})	DON(mg L^{-1})
B1	8.26	32.73	617.12	14.33	223.24	15.99	9.86	4.44	153.88	16.42
B2	9.37	17.84	285.32	4.31	494.02	113.78	12.29	0.79	44.36	0.42
B3	8.98	20.61	647.61	11.42	225.91	19.74	12.43	3.78	55.57	3.15
B4	11.10	9.86	730.52	8.03	222.62	27.84	26.51	21.21	4.05	0.35
B5	11.61	6.03	718.33	9.71	227.21	23.45	29.97	41.81	3.50	0.32
B6	6.98	26.75	122.21	2.02	699.49	387.93	19.04	6.18	31.49	0.28
B7	10.30	6.41	121.31	2.01	783.13	386.61	29.60	15.18	24.85	0.33

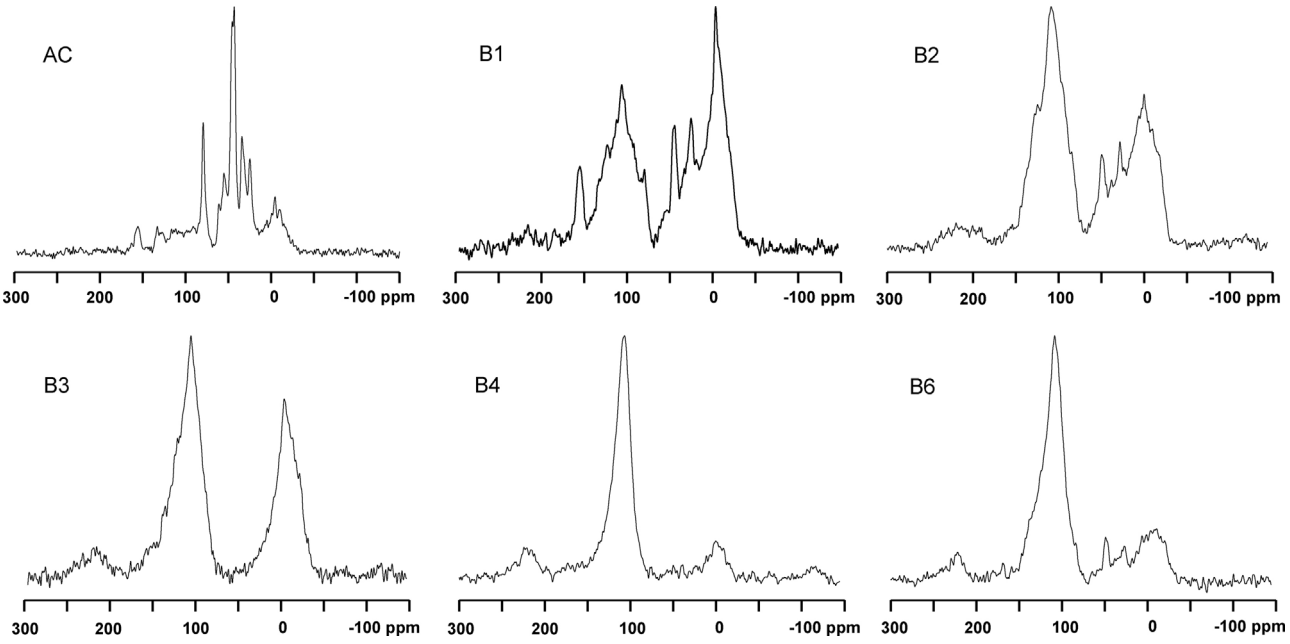

Fig. 1. ^{13}C NMR spectra of alperujo compost (AC) and biochar samples: B1 (BAC_400), B2 (BRH_400), B3 (BAC + BRH_400), B4 (BAC_550), and B6 (BHS).

assignments were interpreted based on characteristic vibrations previously studied for biochars from different feedstock [37,38]. The biochars coating morphologies were observed by using scanning electron microscopy (SEM, Philips XL 30). Biochar samples were previously sputtered with gold in order to improve their conductivity. Solid-state cross-polarization (CP) magic angle spinning (MAS) ^{13}C NMR spectra of all biochar samples were obtained with a Bruker Advance III NMR spectrometer operating at a ^{13}C frequency of 150.91 MHz and a magic-angle-spinning rate of 15 kHz. Between 1600 and 14,000 single scans were accumulated with a pulse delay of 300 ms. The ^{13}C NMR spectra obtained are shown in Fig. 1. A ramped ^{1}H pulse was used during the contact time of 1 ms to circumvent spin modulation during the Hartmann–Hahn contact. The ^{13}C chemical shifts were calibrated relative to tetramethylsilane

Table 4
NMR-data from ^{13}C NMR-spectrum. The resonance frequencies are given as the chemical shift values (ppm). AC (alperujo compost), B1 (BAC_400), B2 (BRH_400), B3 (BAC + BRH_400), B4 (BAC_550), and vB6 (BHS).

Code	250–185	185–160	160–140	140–110	110–90	90–60	60–45	45–70	sum
AC	2.65	3.93	4.5	9.66	11.16	42.46	10.07	15.57	100
B1	4.6	6.41	9.08	22.16	4.85	11.63	9.24	32.02	99.99
B2	5.4	2.48	11.3	32.63	6.26	9.54	7.34	25.03	99.98
B3	7.16	4.71	12.78	34.93	2.89	1.93	3.64	31.96	100
B4	12.36	4.56	11.76	53.5	2.69	2.93	1.89	10.32	100.01
B6	7.63	3.49	14.29	45.61	3.5	5.94	3.74	15.8	100

Table 5
NMR data under consideration of spinning side bands. Polarity index is also given. AC (alperujo compost), B1 (BAC_400), B2 (BRH_400), B3 (BAC + BRH_400), B4 (BAC_550), and B6 (BHS).

Code	Carboxyl C	*O*/*N*-aryl C	H/C-aryl C	*O*-alkyl C	N/methoxyl C	Alkyl C	Sum	Polarity *R*
AC	3.9	4.5	15.0	53.6	10.1	12.9	100.0	2.6
B1	6.4	9.1	31.4	16.5	9.2	27.4	100.0	0.7
B2	2.5	11.3	43.4	15.8	7.3	19.6	100.0	0.6
B3	4.7	12.8	49.3	4.8	3.6	24.8	100.0	0.4
B4	4.6	11.8	78.2	5.6	0.0	0.0	100.2	0.3
B6	3.5	14.3	60.9	9.4	3.7	8.2	100.0	0.4

Table 6
Tricyclazole adsorption–desorption coefficients K_f ($mg^{1-nf}L^{nf}kg^{-1}$) and η_f, R^2 values, k_{d5} (L^{nf}–kg^{-1}) and the hysteresis coefficient (H = η_f ads/η_f des). ALU (alluvial soil), AC (alperujo compost), and B4 (BAC_550).

Samples	$K_f$ads	R^2	$\eta_f$ads	K_{d5}	$K_f$des	R^2	$\eta_f$des	H
ALU	9.26 [922–930]	0.99	0.704 ± 0.003	5.8	15.83 [1550–1617]	0.99	0.87 ± 0.13	0.81
+AC(2%)	12.10 [1102–1328]	0.98	0.530 ± 0.046	5.7	18.13 [1812–1815]	1.00	0.64 ± 0.15	0.83
+B4(2%)	25.02 [2047–3057]	0.95	0.570 ± 0.078	12.5	33.24 [3320–3329]	0.99	0.72 ± 0.08	0.79
+AC(1%) + B4(1%)	17.89 [1521–2104]	0.95	0.498 ± 0.065	8.0	26.87 [2681–2692]	0.99	1.44 ± 0.32	0.35

(0 ppm) with glycine (COOH at 176.08 ppm). The resonance frequencies are given in Table 4. Using MestreNova 9.0 (Mestrelab Research S.L., Santiago de Compostela, Spain) the contributions of the various C groups to the total C were determined by integration of their signal intensity in the respective chemical shift regions (Table 5) under consideration of spinning side band disturbance according to Knicker et al. [39]

Based on the chemical shift differences, the relative intensities were used to calculate the polarity (*R*) (Table 5), which represents the ratio of polar and non-polar groups [40]:

R = (Icarboxy C + Ialky C + IO-ary C)/(IC/H-arylC + Ialky C) Prior to the NMR analysis, the biochar samples were pretreated with hydrochloric acid (HCl) to reduce contributions of paramagnetic components. Therefore, three sets of 2.5 g of each biochar were mixed with 60 ml of 2 M HCl and shaken for 2 h at room temperature. After centrifugation for 10 min at 8000 rpm, the solution was discarded. After repeating the extraction with HCl, the solid residues were washed twice with distilled water and finally oven-dried at 70 °C to a constant weight.

2.4. Fungicide–biochars sorption assays

Tricyclazole adsorption to biochars was studied using a batch technique with fixed sorbent amount (5 mg L^{-1}), in a ratio 0.1:20 (biochar:solution). Based on our preliminary experiments, the sorbent's dosages were adjusted to allow for 20–90% of the added pesticide to be adsorbed at equilibrium. Pesticide solution was prepared with 5 mM $CaCl_2$. According to our preliminary sorption rate and equilibrium studies, it was determined that equilibrium was reached after 16–18 h of biochar–solution contact, and that no measurable degradation occurred during this period. The uptake to the glass walls of centrifuge tubes was negligible. The amount of fungicide adsorbed to the biochars was calculated from the difference between the initial (C_i) and the equilibrium (C_e) solution concentrations.

2.5. Adsorption and desorption of tricyclazole to amended and non-amended soils

Air-dried ALU soil was amended with AC, B4 or a mixture of both: AC (1%) + B4 (1%) at a rate of 2%(w/w). Adsorption isotherms on amended and non-amended soils were measured using a batch equilibration method. Duplicate samples (2.5 g) of unamended and 2%(w/w) amended soils (with AC or B4) were treated with 5 ml of tricyclazole solution with initial concentrations (C_i) ranging from 1.0 to 20 mg L^{-1}. Pesticide solutions were prepared in 5 mM $CaCl_2$. Suspensions were shaken at 20 ± 2 °C for 24 h and centrifuged at 8000 rpm for 10 min. Previously, it was determined that equilibrium was reached in less than 24 h and that no measurable degradation occurred during this period. Supernatants were filtered and C_e values were determined by HPLC. Desorption was accomplished after adsorption using the highest C_i (40 mg L^{-1}) by replacing half of the supernatant with 5 mM $CaCl_2$. This cycle was repeated three times for each sample. Adsorption and desorption isotherms were fitted to the Freundlich equation and the constants K_f and η_f, which indicate the adsorption capacity (evaluated at C_e = 1 mg L^{-1}) and the adsorption intensities respectively, were calculated. The distribution coefficient (K_d) was calculated as the ratio between the amount of pesticide adsorbed at 5 mg L^{-1} (C_{s5}) and C_e, which falls within the range of pesticide concentrations studied. Tricyclazole adsorption–desorption coefficients are presented in Table 6.

2.6. Fungicide extraction and analysis

The concentrations of tricyclazole were determined using a waters 600 E chromatograph coupled to a waters 996 diode-array detector (DAD). The column used was a Nova-Pack C18, 150 × 3.9 mm. Isocratic elution was performed at a flow rate of 1.0 ml/min using the mobile phase of acetonitrile:water (20%:80%). The injection volume was 25 μL for all analysis. Under the used HPLC conditions tricyclazole showed a single peak at the retention time of 6.5 min. Tricyclazole was extracted from soils with methanol and recoveries were close to 100% in all the assays.

External calibration curves were obtained analyzing standard solutions in ultrapure water and acetonitrile at concentrations ranging from 0.05 to 20 mg L^{-1} depending on the analysis. A very high linearity (P_{value} < 0.0001) was always obtained. Quantification was based on chromatographic peak areas. Limits of detection and quantification were assessed observing the signal to noise ratio (S/N) and considering LoD as the concentration with S/N = 3 and LoQ as the concentration with S/N = 10. LoD values were around 0.01 mg L^{-1} for this pesticide. The values of LoQ (concentration) were always around 0.05 mg L^{-1}.

3. Results and discussion

3.1. Elemental composition and physical properties

Physical and chemical properties of the soil, the AC and the soil amended with AC and/or B4 are presented in Table 2. The amendments increased organic matter (OM) contents of the soil, its pH, and its electrical conductivity. The elemental composition of the biochars, atomic ratios (C/N and C/H), physical and chemical properties, and specific surface area are presented in Table 3. Considerable variations of these parameters were observed between biochars due to differences of the feedstock and pyrolysis conditions. The temperature during heating is generally recognized to be the factor which affects most the properties of biochar [41,42]. This is clearly evidenced by comparing biochars of the same feedstock but produced at different temperature (B1, B4, and B5). The BET surface areas of biochars are generally increased with longer residence times and higher temperatures during their production [13]. Comparing B1, B4, and B5, an increase of the SSA of the biochar with increasing temperature is revealed, and has been attributed to the formation of micropores [43]. In addition, a reduction of the SSA of biochars is observed with increasing contents of DOC (Table 3). A similar phenomenon was observed during the sorption of humic substances to char [44]. The model proposed by these authors assumes that humic substances are restricted to the external surface of char where they act as pore blocking agents or competitive adsorbates, depending on the temperature and

adsorbate size. Wen et al. [45] also reported that the coating process of biochars with natural organic matter reduced the SSA of biochars and increased the polarity and aliphaticity. The low BET specific surface area observed in the rice straw biochar ($0.79\ m^2\ g^{-1}$) has been related to its high content of inorganic minerals, which hindered the development of porous C structure [46]. In contrast to black carbon and other plant-derived biochars, wood, and straw charcoals have relatively low surface areas [47]. When we compare B6 and B7, from wood feedstock, we also find higher SSA at higher heat treatment temperature (HTT).

The pH of biochar in solution is generally correlated with the pyrolysis temperature. With higher process intensity, the amount of carboxyl groups in the resulting biochar is reduced and/or the acidic groups are de-protonated to the conjugate bases [42] resulting in a more alkaline pH of the biochar in suspension. Abe et al. [48] indicated that beyond 300 °C, the C starts to volatilize, leading the accumulation of ashes and alkali salts which increases the biochar pH to values above 10. This is in good agreement with the pH values measured for the different biochars studied here: 8.26 (for B1, produced at 400 °C); 10.30 (for B7, produced at >500 °C); 11.10 (for B4, produced at 550 °C); 11.61 (for B5, produced at 700 °C). In addition, the reduction observed in the cation exchange capacity (CEC), was inversely correlated with the HTT of biochar production, as it has been reported previously [12,49].

For the biochars derived from AC, ash contents were high ($731–617\ mg\ g^{-1}$) and carbon contents were low (around $223\ mg\ g^{-1}$). Much lower ash values (around $122\ mg\ g^{-1}$) were obtained for the wood biochars, which also showed the highest carbon contents ($699–783\ mg\ g^{-1}$). The rice hull biochar has an intermediate contribution of ash ($285\ mg\ g^{-1}$). Elevated ash contents in the sample in general increases solution pH [42]. However, we have not observed this for all biochars. Among the studied biochars, those derived from wood showed the highest C/N ratio. On the other side, B4, B5, and B7 presented the highest C/H ratio, thereby indicating a higher aromaticity and condensation as result of the higher temperatures used during their production [50,51].

3.2. ^{13}C NMR spectroscopy

The solid-state ^{13}C NMR spectra of AC and the used biochars are compared in Fig. 1. Their intensity distribution is given in Table 4. The well resolved spectrum of AC reveals its major intensity in the chemical shift region of *O*-alkyl C (110–60 ppm) with typical signals of cellulose. The peak at 56 ppm is most tentatively derived from methoxyl C of lignin but can also embrace signals derived from *N*-alkyl C of peptides. In the chemical shift region of alkyl C (45–0 ppm) the signal at 38 ppm is assignable either to cross linked alkyl C or alkyl C in close vicinity to carboxylic C. The latter results are in resonance lines between 185 and 160 ppm. The signals at 30 and 25 ppm are typical for methylene C. Only low intensity is observed in the aryl-C region (160–110 ppm) but the clear signals at 153 and 148 ppm in the *O*/*N*-aryl-C region (160–140 ppm) confirm the presence of lignin.

As indicated by the spectrum of B4, charring of AC at 550 °C turned the feedstock into a highly aromatic material. However, the shoulder between 140 and 160 ppm contributing with approximately 12% to the total ^{13}C intensity reveals that some aryl C have been oxidized. Such structures are expected to be formed during charring of carbohydrates. With the enhanced aromaticity, the polarity index *R* decreased from 2.6 to 0.3 (Table 5) which is associated to an improved adsorption of hydrophobic compounds. Pyrolyzing AC at 700 °C resulted in a material (B5) which could not be analyzed by solid-state ^{13}C NMR spectroscopy because the irradiation pulse was reflected, assumed to be due to the higher aromatic character [52]. The same was true for B7, produced from wood at a temperature of 700 °C. Lowering the temperature to 500 °C (B6) was sufficient to allow the acquisition of a solid-state ^{13}C NMR spectrum with its main intensity in the C/H-aryl C region. Some intensity is still visible in the *O*-alkyl-C region which is explained with the presence of either protected carbohydrates or carbons in ether bonds. However, in spite of those C groups the polarity index *R* is 0.4. Such a low value was also observed for B3, which according to its ^{13}C NMR spectrum contains a considerable amount of alkyl C. Such spectra are commonly obtained from charcoal derived from N-rich feedstock [53]. Pyrolyzing rice hulls alone at a temperature of 400 °C yielded in a biochar with a spectrum showing aside from the high intensities in the aryl C and alkyl C regions resonance lines assignable to *O*-alkyl C. Its *R* was calculated to be 0.6 and its pattern resembles more that of the spectrum of B1 than that of B3. Here one has to bear in mind that cellulosic material is more efficiently combusted than peptides [53]. For the compost-rice hull mixture this would yield in a biochar which is determined by more difficult to pyrolyze peptide-like constituents. This assumption is supported by the C/N ratios, which is fairly low for B3, but much higher for B2.

3.3. FT-IR spectroscopy

The FT-IR spectra of the biochar samples are given in the Fig. S1 of the Appendix A (Supplementary data). Clear distinctions can be made between the different feedstock and pyrolysis process intensity. Comparing the FT-IR spectra of the biochars derived from AC and obtained at different temperatures (400, 550, and 700 °C), a reduction of the peak intensity of $1070\ cm^{-1}$ (characteristic of C—O stretching of carbohydrate-like substances) and $1470\ cm^{-1}$ (attributed to C—O of phenolic, carboxylic, and alcohol groups) can be observed [45,54]. This reduction is well correlated with the increased pH and CEC values measured for these biochars as a function of increasing production temperature. The loss of OH and aliphatic groups favors the formation of fused-ring structures, especially at higher pyrolysis temperatures [49], which is consistent with the increase in biochar SSA (Table 3). The FT-IR spectra of rice hull biochar, produced at 400 °C (B2), exhibit a peak around $1100\ cm^{-1}$ attributed to the C—O—C symmetric stretching characteristic of cellulose and hemicellulose [55]. In the infrared spectra of the biochar samples produced from wood sawdust (B6) and wood pellet (B7), the intensity of these peaks is very low. The peak observed around $1700\ cm^{-1}$ in the FT-IR spectra of the hardwood sawdust biochar (B6) is assigned to the asymmetric C=O groups, which are generated mainly by dehydration of biopolymers [46,56]. Furthermore, decomposition of hemicelluloses during pyrolysis can be linked to the reduction or disappearance of the 1730 and $1230\ cm^{-1}$ bands, corresponding to acetyl ester groups [57,58].

3.4. Scanning electron microscopy (SEM)

The microphotographs (Fig. 2) revealed that the structure of biochar retain major characteristics of the physical structure of the original feedstock. Similar results have been reported by others [11,59]. The SEM images of the biochars showed remarkable differences in the macroporous (approximately 1 μm diameter) structure and the amount of organic and inorganic matter coated to the char surface. Brodowsky et al. [60] suggested that the more susceptible zones to interactions with both polar organic compounds and the mineral phase observed by SEM are related to reactive functional groups on the surface of the biochar, which are probably *O*-containing groups, such as carboxylic or hydroxylic groups.

3.5. Specific surface area (SSA) assessments

The SSA measured for the biochars (Table 3) is inversely correlated with the contents of DOC, as it was discussed above. This is

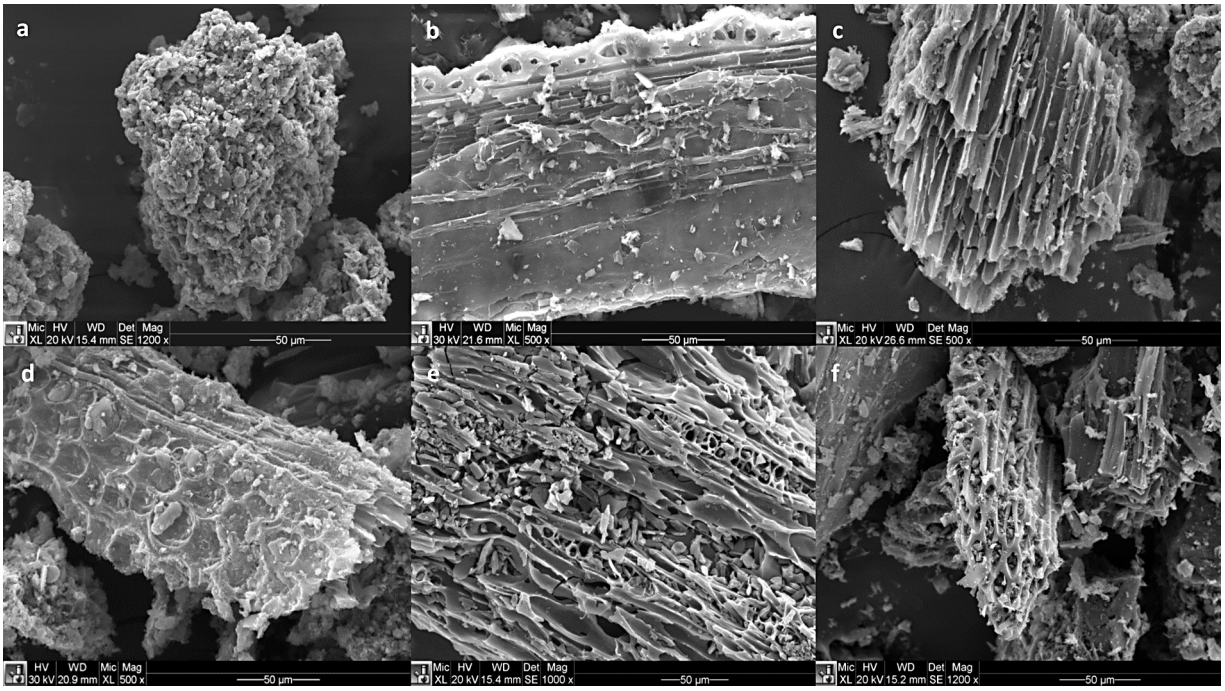

Fig. 2. Scanning electron micrographs of biochar samples: (a) BAC_400, (b) BRH_400, (c) BAC_550, (d) BAC_700,(e) BHS, and (f) BWP.

in good agreement with the SEM images obtained, revealing large differences both with respect to content and location of the residual adsorbed organic matter. Fig. 2c and d, which correspond with B4 and B5, show that very little organic matter is coated to the char surface, whereas Fig. 2a, b, e, and f (B1, B2, B6, and B7) indicate higher amounts of organic matter coating the surface.

3.6. Adsorption and desorption experiments

The adsorption of tricyclazole was previously tested with all the amendments, including the alperujo compost, at the single concentration of 5 ppm. In comparison with AC, the adsorption of tricyclazole on the biochars was always higher, except for the rice hull biochar (Fig. 3). This has been attributed to its very low SSA (0.79 $m^2\ g^{-1}$). The high adsorption values observed are consistent with previous reports on the reaction of xenobiotics with pyrolysis residues derived from natural and anthropogenic sources [61–63]. The lowest values were detected for the mentioned rice hull biochar (B2) and for the hardwood sawdust biochar (B6), which also has a very low SSA (6.18 $m^2\ g^{-1}$). The highest sorption values were observed for B4, B5, and B7 (83.5, 90.3, and 90.7%, respectively). Maximum adsorption of basic pesticides normally occurs at pH levels in the vicinity of the pK_a of the compound [64,65]. However, we observed higher adsorption values in the more alkaline biochar solutions. Therefore, adsorption was mainly related with their high SSA [46,66] and the lower DOC contents measured for these biochars, minimizing the competition between DOC from the biochar and the organic molecule for sorption sites [67].

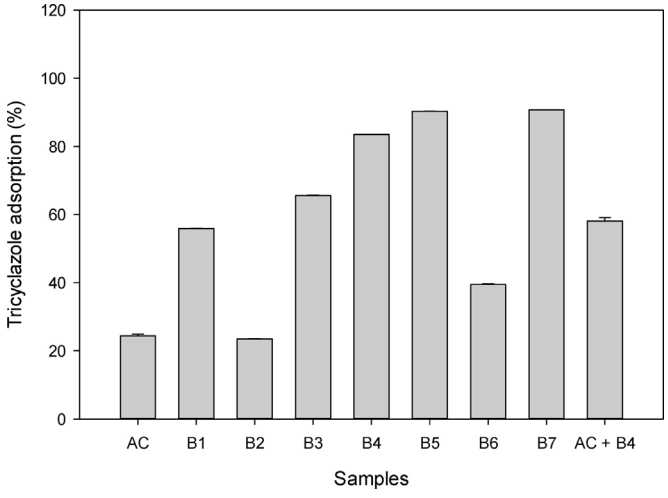

Fig. 3. Tricyclazole adsorption to the amendments. Mean and standard error of two replicates. AC (alperujo compost), B1 (BAC_400), B2 (BRH_400), B3 (BAC + BRH_400), B4 (BAC_550), B5 (BAC_700), B6 (BHS), B7 (BWP), and AC + B4 (alperujo compost + BAC_550).

Of the seven biochars assessed, B4, which had similar sorption properties to B5, and was produced at lower HTT, was selected to be compared and mixed with AC in order to evaluate its potential to improve soil properties and reduce the mobility of tricyclazole in paddy soils without affecting its biological activity, i.e., enhancing reversible sorption processes.

The adsorption–desorption isotherms of tricyclazole by the ALU soil with and without amendments (AC, B4, and AC + B4) are shown in Fig. 4. Sorption data fitted very well to the Freundlich equation, with R^2 values from 0.95 to 1.00 (Table 6). Non-linear isotherms are observed due to a Langmuir-type adsorption, characterized by the strong interaction between adsorbent and adsorbate. Similar behavior was described for other triazole fungicides [23], where the adsorption decreased as the aqueous concentration of pesticide increased. The isotherms exhibit increasing non-linearity with AC, B4, and the mixture amendment, corresponding to the increasing deviation from one of η_f values in the Freundlich model (Table 6). This suggests a significant solute adsorption on a small amount of a high-surface area material in soil and to specific interactions of tricyclazole with highly reactive sites provided for the organic matter from the amendment, supporting previous results obtained with other amendments and other sorbents [61,68]. The curvilinear isotherm indicates that the number of available sites for the adsorption turned into a limiting factor at the higher concentrations of tricyclazole. Though the OC content in the soil is usually

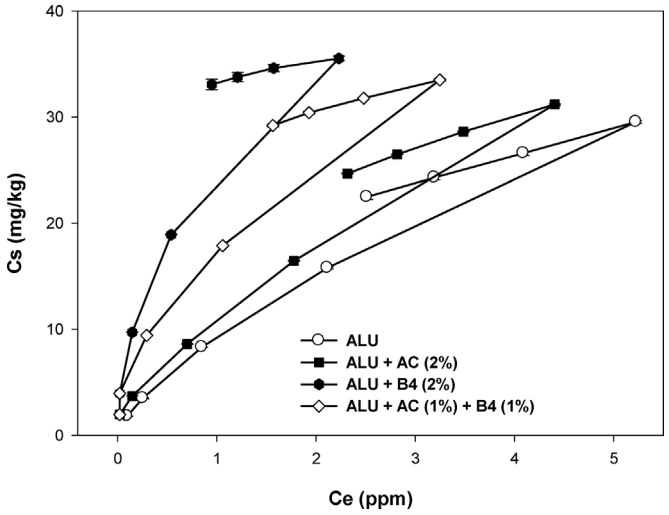

Fig. 4. Tricyclazole adsorption–desorption isotherms for the alluvial soil with the different amendments. Mean and standard error of three replicates. ALU (alluvial soil), ALU + AC (alluvial soil + alperujo compost), ALU + B4 (alluvial soil + BAC_550), and ALU + AC + B4 (alluvial soil + alperujo compost + BAC_550).

recognized as the parameter which most affects the adsorption of triazole fungicides [23], we have to bear in mind the higher adsorption capacity of the exogenous OM of the amended soils, as has been previously reported [69,70]. This mobile fraction may be responsible of the lowest adsorption value observed in the soil amended with AC. The soil amended with B4 (2% w/w) shows the highest adsorption of tricyclazole over the entire range of the tested solution concentrations, with a medium η_f value (0.570) and the highest K_f value (25.02) of the adsorption isotherms. This is best explained with the higher SSA of this biochar [24]. No significant relationship between the pH of the suspensions with amended and non-amended soils and the adsorption values were found. Intermediate adsorption values (K_{fads} and K_d) were observed for the soil amended with a mixture of AC and B4. However, the most interesting finding is the much lower hysteresis coefficient value, indicating the higher reversibility of the AC–B4 mixture when compared to AC or B4. These results indicate that under paddy field conditions, soil amended with a mixture of AC and B4 can increase sorption of tricyclazole. This reduces the risk of transport through leaching or runoff without impeding its subsequent release, due to the high reversibility of the process.

4. Conclusions

This study provides direct experimental evidence of the effectiveness of the selected biochars in the retention of tricyclazole in a water saturated soil. Particular biochar amendments could be beneficial for the remediation of polluted soils or for the prevention of tricyclazole leaching in paddy field conditions, but would also entail a reduction of the efficacy of the applied pesticide. These results also stress the importance of proper screening of biochar characteristics before application. Based on adsorption–desorption data, we recommend the use of a mixture of alperujo compost and biochar produced from the same compost at 550 °C for optimal efficiency of tricyclazole, while minimizing the risk of contamination of superficial and ground-water under flooded conditions.

Acknowledgments

This research was supported by the Ministry of Economy and Competitiveness (AGL2010-21421 and AGL2013-48446-C3-1-R) and the Autonomous Government of Andalusia (PAIDI AGR-264). The projects were co-financed with European funds (FEDER-FSE PO2007-13). Manuel García-Jaramillo thanks MEC/FECYT for a doctoral fellowship through AGL2010-21421-CO2-01 project of MICINN. Further, we would like to thank to the Analytical Service of the IRNAS (CSIC) and to the Center of Research Technology and Innovation of the University of Seville (CITIUS) for their technical assistance.

Appendix A. Supplementary data

Supplementary data associated with this article can be found, in the online version, at http://dx.doi.org/10.1016/j.jhazmat.2014.10.052.

References

[1] J. Fernández-Bayo, R. Nogales, E. Romero, Assessment of three vermicomposts as organic amendments used to enhance diuron sorption in soils with low organic carbon content, Eur. J. Soil Sci. 60 (2009) 935–944.
[2] D. Gondar, R. López, J. Antelo, S. Fiol, F. Arce, Effect of organic matter and pH on the adsorption of metalaxyl and penconazole by soils, J. Hazard. Mater. 260 (2013) 627–633.
[3] M. García-Jaramillo, L. Cox, J. Cornejo, M.C. Hermosín, Effect of soil organic amendments on the behavior of bentazone and tricyclazole, Sci. Total Environ. 466–467 (2014) 906–913.
[4] J.W. Lee, M. Kidder, B.R. Evans, S. Paik, A.C. Buchanan III, C.T. Garten, R.C. Brown, Characterization of biochars produced from cornstovers for soil amendment, Environ. Sci. Technol. 44 (2010) 7970–7974.
[5] D.A. Laird, The charcoal vision: a win–win–win scenario for simultaneously producing bioenergy permanently sequestering carbon, while improving soil and water quality, Agron. J. 100 (2008) 178–181.
[6] K.A. Spokas, W.C. Koskinen, J.M. Baker, D.C. Reicosky, Impacts of woodchip biochar additions on greenhouse gas production and sorption/degradation of two herbicides in a Minnesota soil, Chemosphere 77 (2009) 574–581.
[7] J. Wang, M. Zhang, Z. Xiong, P. Liu, G. Pan, Effects of biochar addition on N_2O and CO_2 emissions from two paddy soils, Biol. Fertil. Soils 47 (2011) 887–896.
[8] D.C. Case Sean, N.P. McNamara, D.S. Reay, J. Whitaker, The effect of biochar addition on N_2O and CO_2 emissions from a sandy loam soil – the role of soil aeration, Soil Biol. Biochem. 51 (2012) 125–134.
[9] J. Lehmann, Bioenergy in the black, Front. Ecol. Environ. 5 (2007) 381–387.
[10] J.J. Manyà, Pyrolysis for biochar purposes: a need to establish current knowledge gaps and research needs, Environ. Sci. Technol. 46 (2012) 7939–7954.
[11] S.P. Sohi, E. Krull, E. Lopez-Capel, R. Bol, A review of biochar and its use and function in soil Advances in Agronomy, vol. 105, Academic Press, Burlington, 2010, pp. 47–82.
[12] B. Singh, B.P. Singh, A.L. Cowie, Characterization and evaluation of biochars for their application as a soil amendment, Aust. J. Soil Res. 48 (2010) 516–525.
[13] C.E. Brewer, R. Unger, K. Schmidt-Rohr, R.C. Brown, Criteria to select biochars for fieldstudies based on biochar chemical properties, Bioenerg. Res. 4 (2011) 312–323.
[14] K.Y. Chan, L. Van Zwieten, I.A. Meszaros, A. Downie, S. Joseph, Agronomic values of green waste as a soil amendment, Aust. J. Soil Res. 45 (2007) 629–634.
[15] L. Van Zwieten, S. Kimber, S. Morris, K.Y. Chan, A. Downie, J. Rust, S. Joseph, A. Cowie, Effects of biochar and slow pyrolysis of papermill waste on agronomic performances and soil fertility, Plant Soil 327 (2010) 235–246.
[16] J.M. Novak, W.J. Busscher, D.W. Watts, J.E. Amonette, J.A. Ippolito, I.M. Lima, J. Gaskin, K.C. Das, C. Steiner, M. Ahmedna, D. Rehrah, H. Schomberg, Biochars impact on soil-moisture storage in an ultisol and two aridisols, Soil Sci. 177 (2012) 310–320.
[17] J. Lehmann, M. Rillig, J. Theis, C.A. Masiello, W.C. Hockaday, D. Crowley, Biochar effects on soil biota: a review, Soil Biol. Biochem. 43 (2011) 1812–1836.
[18] Y. Yang, G. Sheng, Enhanced pesticide sorption by soils containing particulate matter from crop residue burns, Environ. Sci. Technol. 37 (2003) 3635–3639.
[19] V.A. Loganathan, Y. Feng, G.D. Sheng, T.P. Clement, Crop-residue-derived char influences sorption: desorption and bioavailability of atrazine in soils, Soil Sci. Soc. Am. J. 73 (2009) 967–974.
[20] R.S. Kookana, The role of biochar in modifying the environmental fate bioavailability, and efficacy of pesticides in soils: a review, Aust. J. Soil Res. 48 (2010) 627–637.
[21] J. Lehmann, S. Joseph, Biochar for Environmental Management, Science and Technology, Earthscan Publisher, London, U.K, 2009.
[22] A. Enders, K. Hanley, T. Whitman, S. Joseph, J. Lehmann, Characterization of biochars to evaluate recalcitrance and agronomic performance, Bioresour. Technol. 114 (2012) 644–653.
[23] N. Singh, Sorption behavior of triazole fungicides in indian soils and its correlation with soil properties, J. Agric. Food Chem. 50 (2002) 6434–6439.

[24] E.R. Graber, L. Tsechansky, J. Khanukov, Y. Oka, Sorption volatilization, and efficacy of the fumigant 1,3-dichloropropene in a biochar-amended soil, Soil Sci. Soc. Am. J. 75 (2011) 1365–1373.
[25] A. Cabrera, L. Cox, K. Spokas, M.C. Hermosín, J. Cornejo, W.C. Koskinen, Comparative sorption and leaching study of the herbicides fluometuron and MCPA in a soil amended with biochars and other sorbents, J. Agric. Food Chem. 59 (2011) 12550–12560.
[26] X. Yu, L. Pan, G. Ying, R.S. Kookana, Enhanced and irreversible sorption of pesticide pyrimethanil by soil amended with biochars, J. Environ. Sci. 22 (2010) 615–620.
[27] R.H. Bromilow, A.A. Evans, P.H. Nicholls, Factors affecting degradation rates of five triazole fungicides in two soil types: 1 laboratory incubations, Pestic. Sci. 55 (1999) 1129–1134.
[28] L. Padovani, E. Capri, C. Padovani, E. Puglisi, M. Trevisan, Monitoring tricyclazole residues in rice paddy watersheds, Chemosphere 62 (2006) 303–314.
[29] The Pesticide Manual, in: C. Tomlin (Ed.), 14th ed., British Crop Protection Council, Farnham, Surrey, 2006.
[30] H.X. Zhang, X. Huang, P. Mei, K.H. Li, C.N. Yan, Studies on the interaction of tricyclazole with β-cyclodextrin and human serum albumin by spectroscopy, J. Fluoresc. 16 (2006) 287–294.
[31] I.W.G. WRB, World Reference Base for Soil Resources, FAO, Rome, 2006.
[32] G.W. Gee, J.W. Bauder, Particle-size analysis. In; Klute, A., Dinauer, R. C., Eds.; Soil. Sci. Soc. Am. J., Madison Methods of soil analysis Part 1, 2nd, WI. 1986; 383-409.
[33] B.H. Sheldrick, C. Wang, Particle-size distribution, in: M.R. Carter (Ed.), Soil Sampling and Methods of Analysis, Lewis Publishers, Ann Arbor, MI, 1993, pp. 499–511.
[34] A. Walkley, J.A. Black, An examination of the degtjareff method for determining soil organic matter, and proposed modification of the chromic acid titration method, Soil Sci. 37 (1934) 29–38.
[35] J.J. Benton, Kjeldahl Method for Nitrogen Determination, Micro-Macro Publishing, Athens, GA, 1991.
[36] S. Brunauer, P.H. Emmett, E. Teller, Adsorption of Gases in Multimolecular Layers Contribution, The Bureau of Chemistry and Soils and George Washington University, 1938, pp. 309–319.
[37] X. Cao, W. Harris, Properties of dairy-manure-derived biochar pertinent to its potential use in remediation, Bioresour. Technol. 101 (2010) 5222–5228.
[38] K.B. Cantrell, P.G. Hunt, M. Uchimiya, J.M. Novak, K.S. Ro, Impact of pyrolysis temperature and manure source on physicochemical characteristics of biochar, Bioresour. Technol. 107 (2012) 419–428.
[39] H. Knicker, K.U. Totsche, G. Almendros, F.J. González-Vila, Condensation degree of burnt peat and plant residues and the reliability of solid-state VACP MAS ^{13}C NMR spectra obtained from pyrogenic humic material, Org. Geochem. 36 (2005) 1359–1377.
[40] K. Abelmann, S. Kleineidam, H. Knicker, P. Grathwohl, I. Kögel-Knabner, Sorption of HOC in soils with carbonaceous contamination: influence of organic matter composition, J. Plant Nutr. Soil Sci. 168 (2005) 293–306.
[41] H. Sun, W.C. Hockaday, C.A. Masiello, K. Zygourakis, Multiple controls on the chemical and physical structure of biochars, Ind. Eng. Chem. Res. 51 (2012) 3587–3597.
[42] F. Ronsse, S. Van Hecke, D. Dickinson, W. Prins, Production and characterization of slow pyrolysis biochar: influence of feedstock type and pyrolysis conditions, GCB Bioenergy 5 (2013) 104–115.
[43] M.I. Bird, P.L. Ascough, I.M. Young, C.V. Wood, A.C. Scott, X-ray microtomographic imaging of charcoal, J. Archaeol. Sci. 35 (2008) 2698–2706.
[44] J.J. Pignatello, S. Kwon, Y. Lu, The effect of natural organic substances on the surface and adsorptive properties of environmental black carbon (Char): attenuation of surface activity by humic and fulvic acids, Environ. Sci. Technol. 40 (2006) 7757–7763.
[45] B. Wen, R. Huang, R. Li, P. Gong, S. Zhang, Z. Pei, J. Fang, X.Q. Shan, S.U. Khan, Effects of humic acid and lipid on the sorption of phenanthrene on char, Geoderma 150 (2009) 202–208.
[46] J. Lü, J. Li, Y. Li, B. Chen, Z. Bao, Use of rice straw biochar simultaneously as the sustained release carrier of herbicides and soil amendment for their reduced leaching, J. Agric. Food Chem. 60 (2012) 6463–6470.
[47] M.B. Fernandes, P. Brooks, Characterization of carbonaceous combustion residues: II Nonpolar organic compounds, Chemosphere 53 (2003) 447–458.
[48] I. Abe, S. Iwasaki, Y. Iwata, H. Kominami, Y. Kera, Relationship between production method and adsorption property of charcoal, Tanso 185 (1998) 277–284.
[49] S. Kloss, F. Zehetner, A. Dellantonio, R. Hamid, F. Ottner, V. Liedtke, M. Schwanninger, M.H. Gerzabek, G. Soja, Characterization of slow pyrolysis biochars: effects of feedstocks and pyrolysis temperature on biochar properties, J. Environ. Qual. 41 (2012) 990–1000.
[50] K.J. Brown, J.S. Clark, E.C. Grimm, J.J. Donovan, P.G. Mueller, B.C.S. Hansen, I. Stefanova, Fire cycles in North American interior grasslands and their relation to prairie drought, Proc. Natl. Acad. Sci. 102 (2005) 8865–8870.
[51] M. Keiluweit, P.S. Nico, M.G. Johnson, M. Kleber, Dynamic molecular structure of plant biomass-derived black carbon (biochar), Environ. Sci. Technol. 44 (2010) 1247–1253.
[52] H. Knicker, Solid state CPMAS ^{13}C and ^{15}N NMR spectroscopy in organic geochemistry and how spin dynamics can either aggravate or improve spectra interpretation, Org. Geochem. 42 (2011) 867–890.
[53] H. Knicker, Black nitrogen – an important fraction in determining the recalcitrance of charcoal, Org. Geochem. 41 (2010) 947–950.
[54] H. Dong, F. Li, J. Li, Y. Li, Characterizations of blend gels of carboxymethylated polysaccharides and their use for the controlled release of herbicide, J. Macromol. Sci. Chem. 49 (2012) 235–241.
[55] W. Wu, M. Yang, Q. Feng, K. McGrouther, H. Wang, H. Lu, Y. Chen, Chemical characterization of rice straw-derived biochar for soil amendment, Biomass Bioenerg. 47 (2012) 268–276.
[56] R.K. Sharma, J.B. Wooten, V.L. Baliga, X. Lin, W. Geoffrey Chan, M.R. Hajaligol, Characterization of chars from pyrolysis of lignin, Fuel 83 (2004) 1469–1482.
[57] M. Schwanninger, J.C. Rodrigues, H. Pereira, B. Hinterstoisser, Effects of short-time vibratory ball milling on the shape of FT-IR spectra of wood and cellulose, Vib. Spectrosc. 36 (2004) 23–40.
[58] B. Stefke, E. Windeisen, M. Schwanninger, B. Hinterstoisser, Determination of the weight percentage gain and of the acetyl group content of acetylated wood by means of different infrared spectroscopic methods, Anal. Chem. 80 (2008) 1272–1279.
[59] J. Laine, S. Yunes, Effect of the preparation method on the pore size distribution of activated carbon from coconut shell, Carbon 30 (1992) 601–604.
[60] S. Brodowski, W. Amelung, L. Haumeier, C. Abetz, W. Zech, Morphological and chemical properties of black carbon in physical soil fractions as revealed by scanning electron microscopy and energy-dispersive X-ray spectroscopy, Geoderma 128 (2005) 116–129.
[61] B. Chen, D. Zhou, L. Zhu, Transitional adsorption and partition of nonpolar and polar aromatic contaminants by biochars of pine needles with different pyrolytic temperatures, Environ. Sci. Technol. 42 (2008) 5137–5143.
[62] K. Sun, M. Keiluweit, M. Kleber, Z. Pan, B. Xing, Sorption of fluorinated herbicides to plant biomass-derived biochars as a function of molecular structure, Bioresour. Technol. 102 (2011) 9897–9903.
[63] J. Li, Y. Li, M. Wu, Z. Zhang, J. Lü, Effectiveness of low-temperature biochar in controlling the release and leaching of herbicides in soil, Plant Soil 370 (2013) 333–344.
[64] J.B. Weber, Interaction of organic pesticides with particulate matter in aquatic and soil systems, in: In Fate of Organic Pesticides in the Aquatic Environment. Advances in Chemistry Series, Number III, American Chemical Society, USA, 1972, pp. 55–120.
[65] J.B. Weber, Ionization and adsorption-desorption of tricyclazole by soil organic matter: montmorillonite clay and Cape Fear sandy loam soil, J. Agric. Food Chem. 30 (1982) 584–588.
[66] X.B. Yang, G.G. Ying, P.A. Peng, L. Wang, J.L. Zhao, L.J. Zhang, P. Yuan, H.P. He, Influence of biochars on plant uptake and dissipation of two pesticides in an agricultural soil, J. Agric. Food Chem. 58 (2010) 7915–7921.
[67] A. Cabrera, L. Cox, K. Spokas, M.C. Hermosín, J. Cornejo, W.C. Koskinen, Influence of biochar amendments on the sorption–desorption of aminocyclopyrachlor, bentazone and pyraclostrobin pesticides to an agricultural soil, Sci. Total Environ. 470 (471) (2014) 438–443.
[68] L. Cox, M.C. Fernandes, A. Zsolnay, M.C. Hermosín, J. Cornejo, Changes in dissolved organic carbon of soil amendments with aging: effect on pesticide adsorption behavior, J. Agric. Food Chem. 52 (2004) 5635–5642.
[69] L. Cox, R. Celis, M.C. Hermosín, J. Cornejo, A. Zsolnay, K. Zeller, Effect of organic amendments on herbicide sorption as related to the nature of the dissolved organic matter, Environ. Sci. Technol. 34 (21) (2000) 4600–4605.
[70] M.C. Fernandes, L. Cox, M.C. Hermosín, J. Cornejo, Organic amendments affecting sorption, leaching and dissipation of fungicides in soils, Pest Manage. Sci. 62 (2006) 1207–1215.